TFAWS Passive Thermal Paper Session

Thermal radiation in the cryogenic regime

NASA Glenn Research Center
Thermal Systems Branch (LTT)

Presented By

Justin P. Elchert

Thermal & Fluids Analysis Workshop
TFAWS 2018
August 20-24, 2018
NASA Johnson Space Center
Houston, TX

Topics

- Review of multilayer insulation (also called superinsulation) fundamentals
  - Types of MLI models
- Introduction of advanced concepts
  - Non-gray
  - Seams
  - Validating Thermal Desktop
- Incoporating these concepts into Thermal Desktop models
- Discussion of results

Types of MLI models

- Numerical (commercial code, or custom code)
- Floating shields analytical model

$$q = \frac{\sigma(T_1^4 - T_2^4)}{1/\epsilon_1 + 1/\epsilon_2 - 1 + \sum_{n=1}^{N-1}(1/\epsilon_{n2} + 1/\epsilon_{(n+1)1} - 1) + 1/\epsilon_{N2} + 1/\epsilon_2 - 1} \quad (22)$$

- Semi-empirical models

$$q = \frac{c''}{t}\overline{N}^m T_m(T_h - T_c) + \frac{3}{7}\frac{b_2 n^3 \sigma}{N_o}(T_h^{14/3} - T_c^{14/3}) \quad (38)$$

- Polynomial fits

$$q = h(T_h - T_c) + \epsilon'_{eff}\sigma(T_h^4 - T_c^4)$$

$$q = c_3(T_h^2 - T_c^2) + c_4(T_h^3 - T_c^3) + c_5(T_h^4.67 - T_c^4.67)$$

- Iterative separated mode

Validation case: floating shields

Analytical solution	Thermal Desktop solution
90	90.0000
128.494	128.9190
147.986	148.4690
161.873	162.3760
172.896	173.4180
182.14	182.6130
190.159	190.5390
197.275	197.5990
203.695	203.9480
209.56	209.7310
214.97	215.0610
220	220.0000

-5.34 W/m^2 **-5.34 W/m^2**

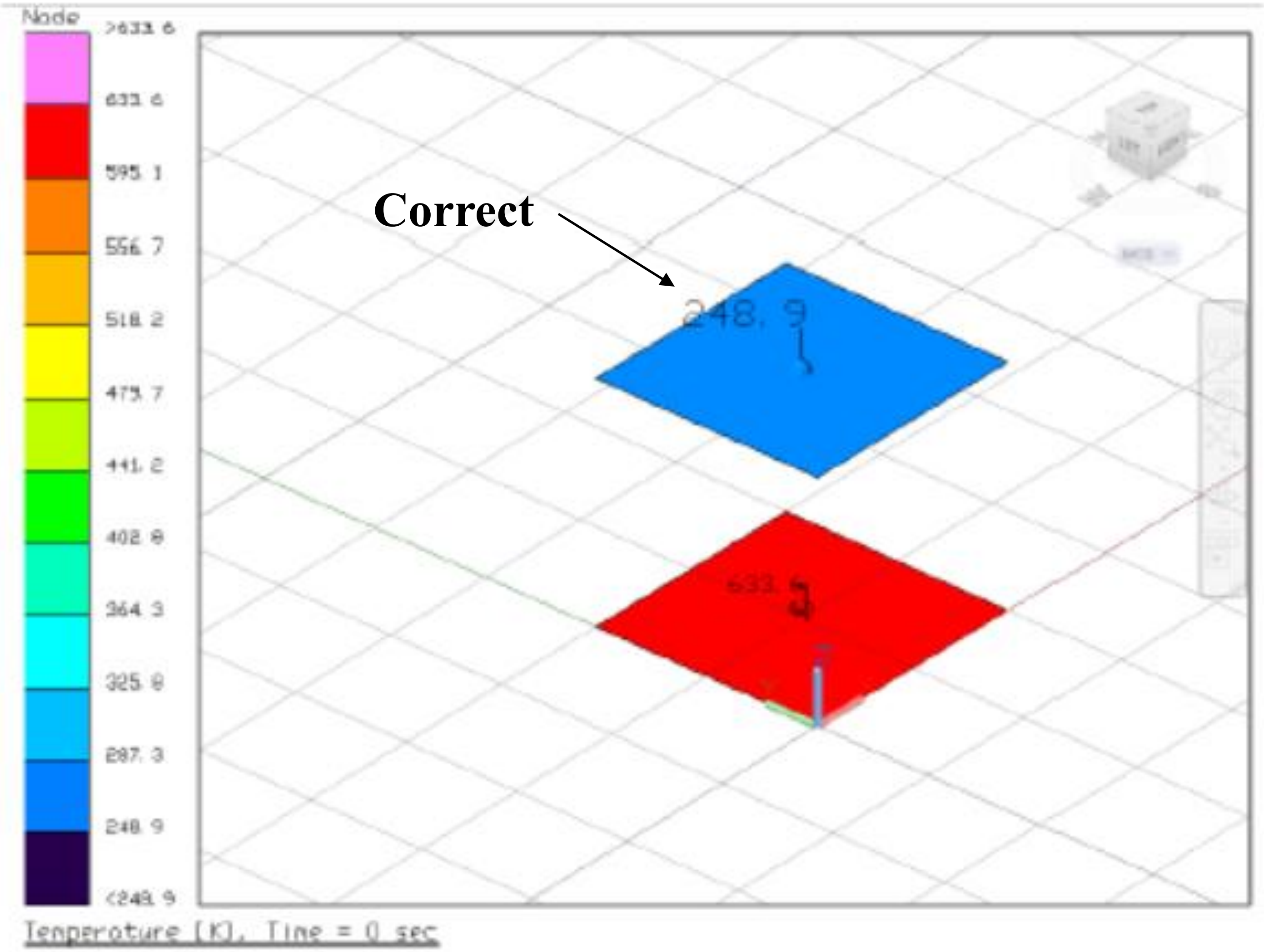

Node
>633.6
633.6
595.1
556.7
518.2
479.7
441.2
402.8
364.3
325.8
287.3
248.9
<248.9
Correct
248.9
Temperature [K], Time = 0 sec

Reminder: check ray tracing assumptions

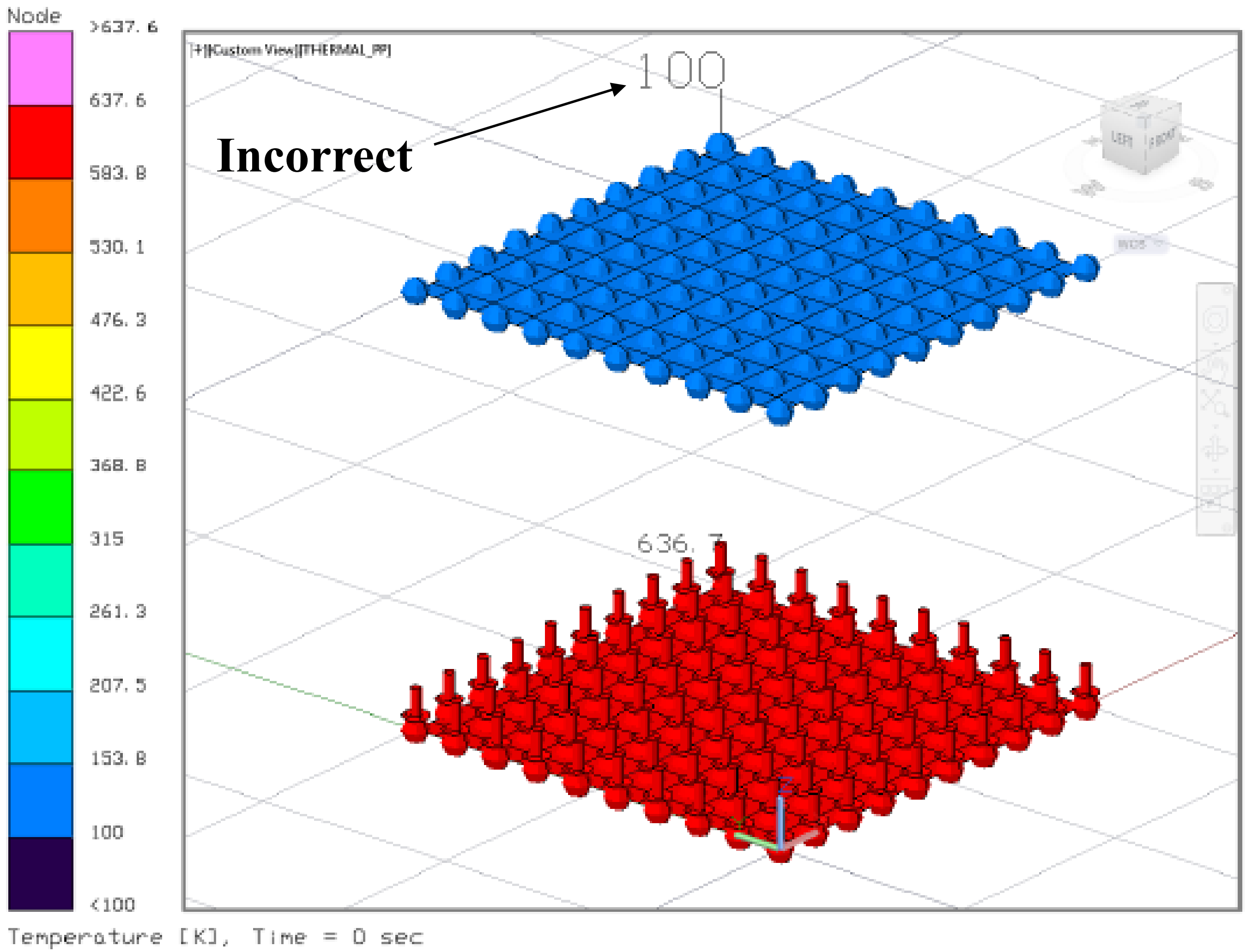

Review: the gray surface

- **A gray surface has the simplifying property that the absorptivity may be reasonably assumed to equal the emissivity**

Pre-requisites

1. **Either the irradiation is diffuse or the surface is diffuse**
2. **Spectral properties of surface are nearly constant over spectral region of interest**
3. **Irradiation and surface emission occur in the bounds of the spectral region of interest**

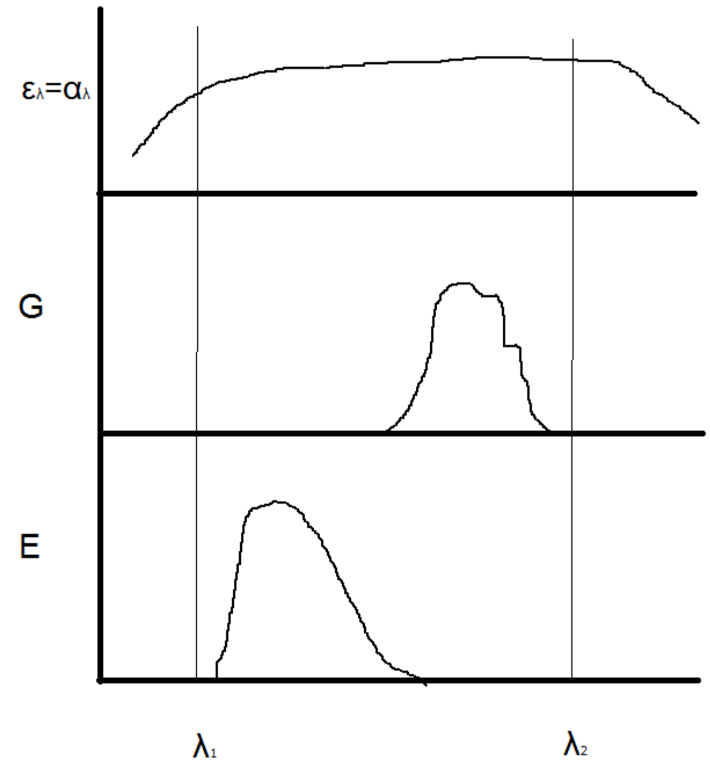

$$\epsilon(T) = \frac{\int_0^{\infty} \epsilon_\lambda(\lambda, T) E_{\lambda_b}(\lambda, T) d\lambda}{E_b(T)}$$

Non-gray validation case

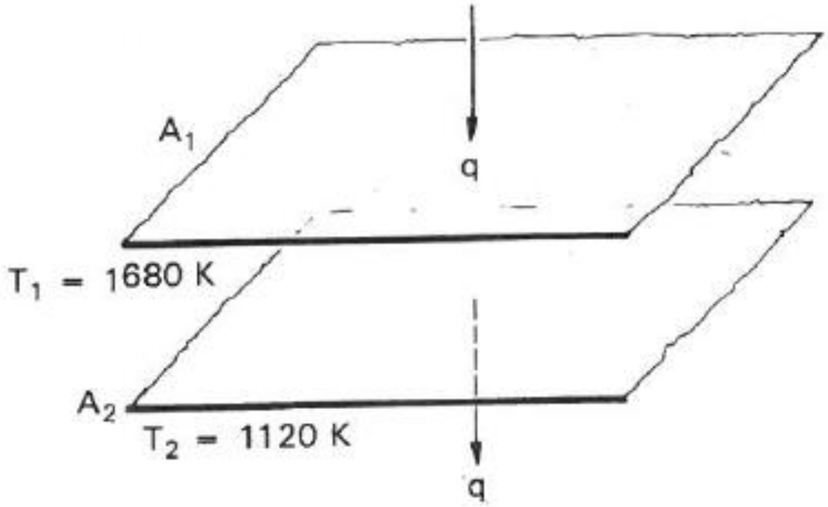

Siegel & Howell

Problem 8-2

Solution: 140,500 W/m^2

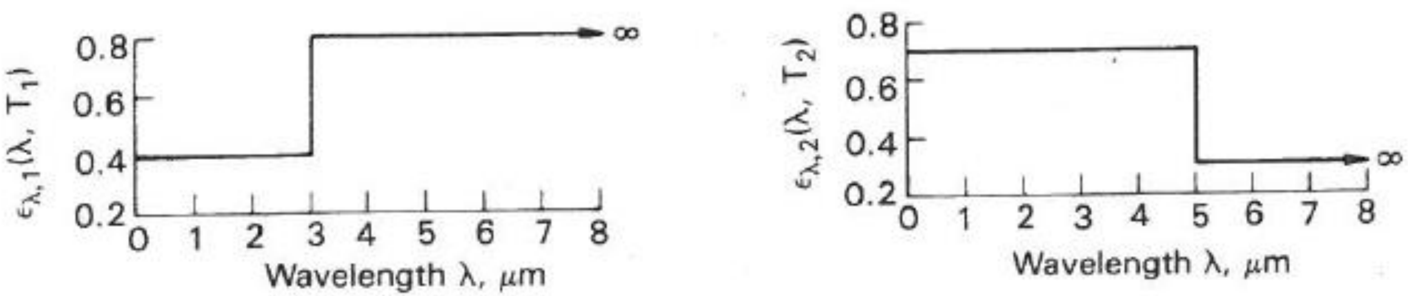

Figure 8-4 Example of heat transfer across space between infinite parallel plates having spectrally dependent emissivities.

Non-gray validation case

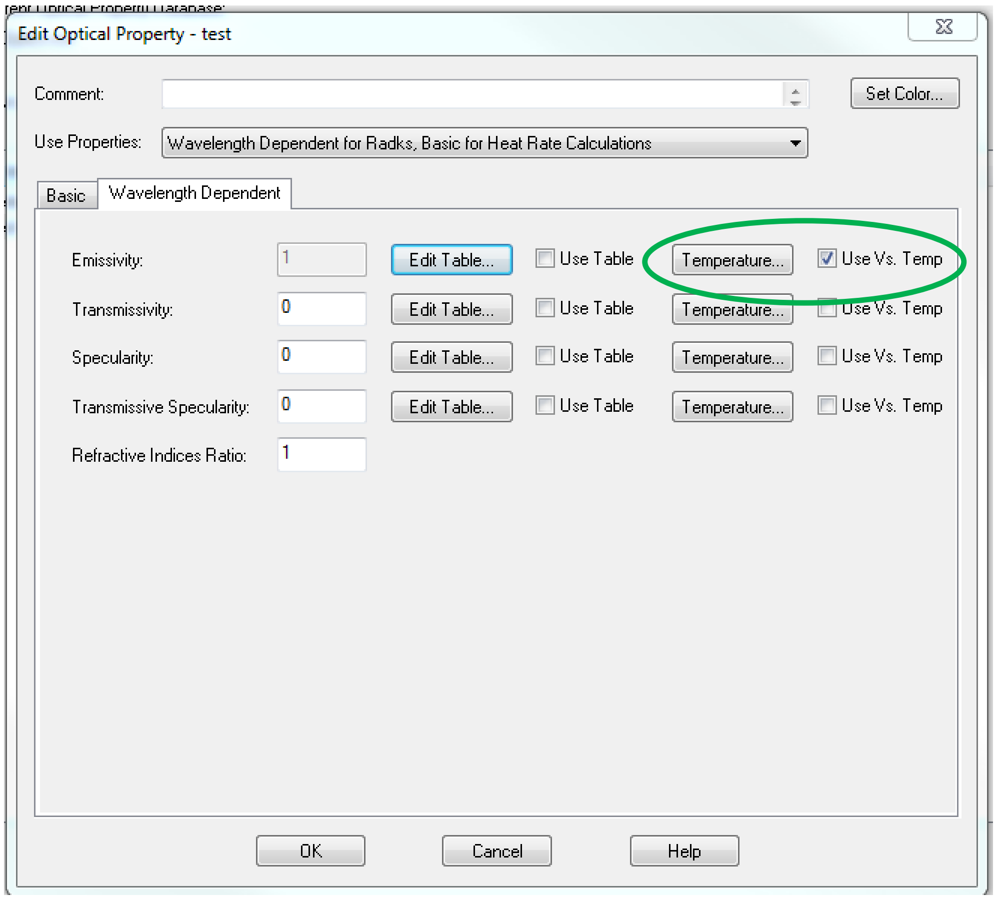

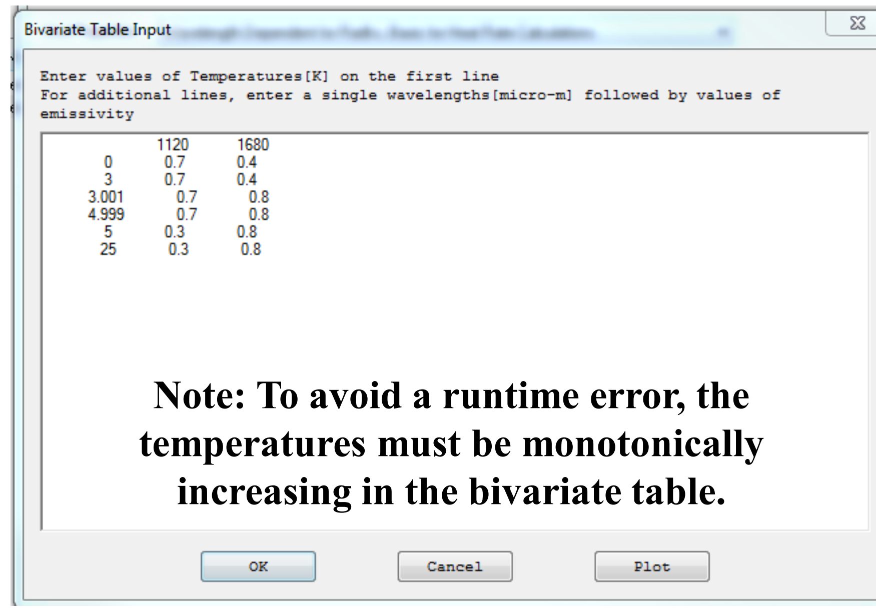

Note: To avoid a runtime error, the temperatures must be monotonically increasing in the bivariate table.

Non-gray validation case

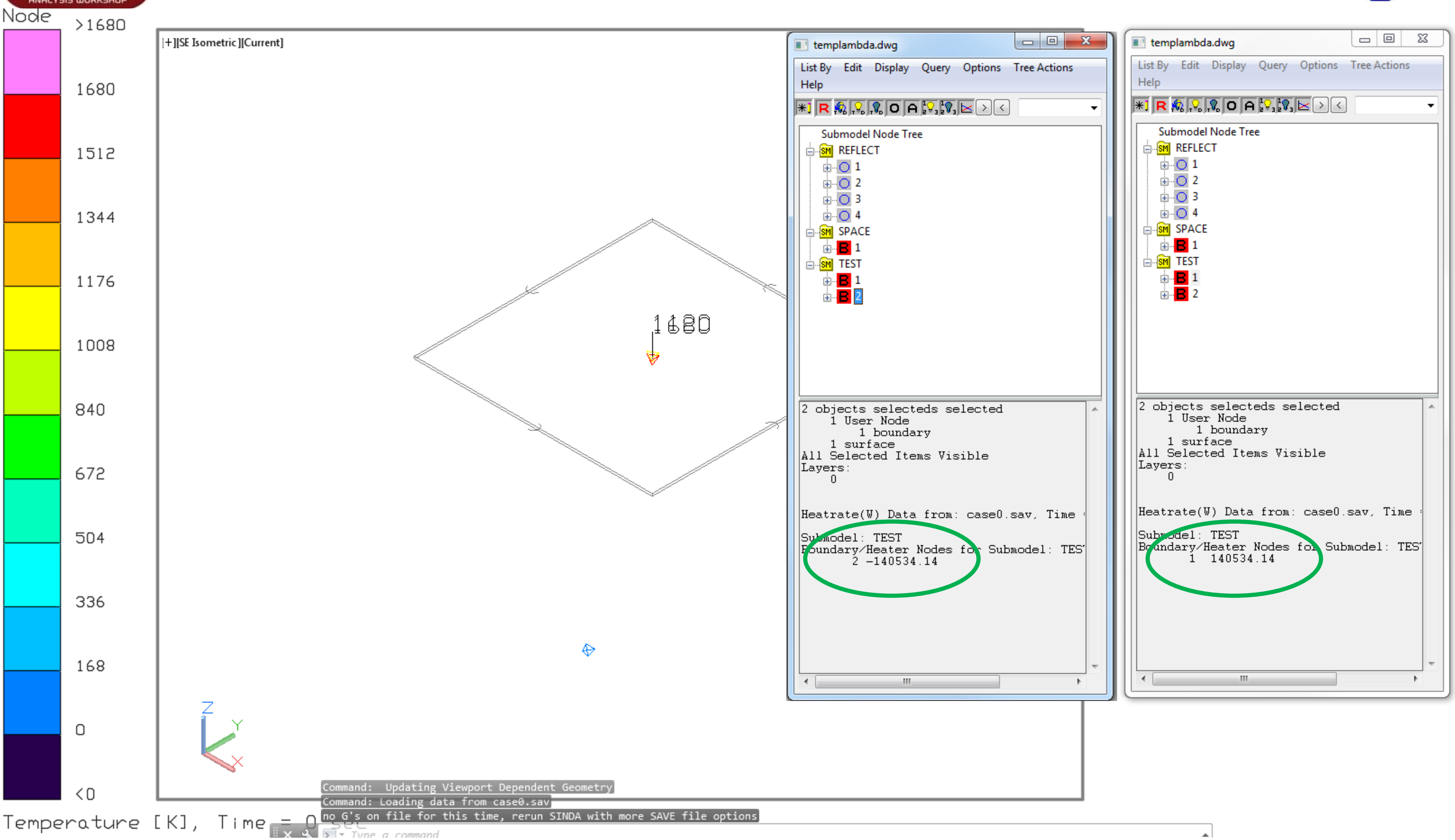

Srinivasan's Paradox

- J. Srinivasan [24] observed that their dewar suffered roughly **66% more heat leak** when filled with LN2 than with LH2 (no blanket, just a thermos type setup)
- I.A. Black and P.E. Glaser [27] reported **41% more heat transfer** with a 1 inch thick blanket in their 35-liter dewar
- **What's going on here? The hydrogen is colder and the surroundings are the same temperature. Why is liquid nitrogen losing more heat?**

Srinivasan's approach (Hagen-Rubens eq)

$$n = \kappa = \sqrt{\frac{\lambda_o \mu_o c_o}{4\pi r_e}} = \sqrt{\frac{0.003\lambda_o}{r_e}}$$

$$\epsilon'_n = \frac{4n}{(n+1)^2 + \kappa^2} \implies \epsilon'_{\lambda,n}(\lambda) = \frac{4n}{2n^2 + 2n + 1} = \frac{2}{n} - \frac{2}{n^2} + \frac{1}{n^3} - \frac{1}{2n^5} + \frac{1}{2n^6} - \ldots$$

$$\epsilon'_n(\lambda) = \frac{2}{\sqrt{0.003}}\sqrt{\frac{r_e}{\lambda_o}} - \frac{2}{0.003}\frac{r_e}{\lambda_o} + \ldots \approx 36.5\sqrt{\frac{r_e}{\lambda_o}} - 464\frac{r_e}{\lambda_o}$$

$$\therefore \quad q(T_1, T_2) = \int_5^{10000} \frac{E_{\lambda_b}(\lambda, T_1) - E_{\lambda_b}(\lambda, T_2)}{\frac{1}{\epsilon_h(\lambda, T_1)} + \frac{1}{\epsilon_h(\lambda, T_2)} - 1} d\lambda$$

Hagen-Rubens derived emissivity

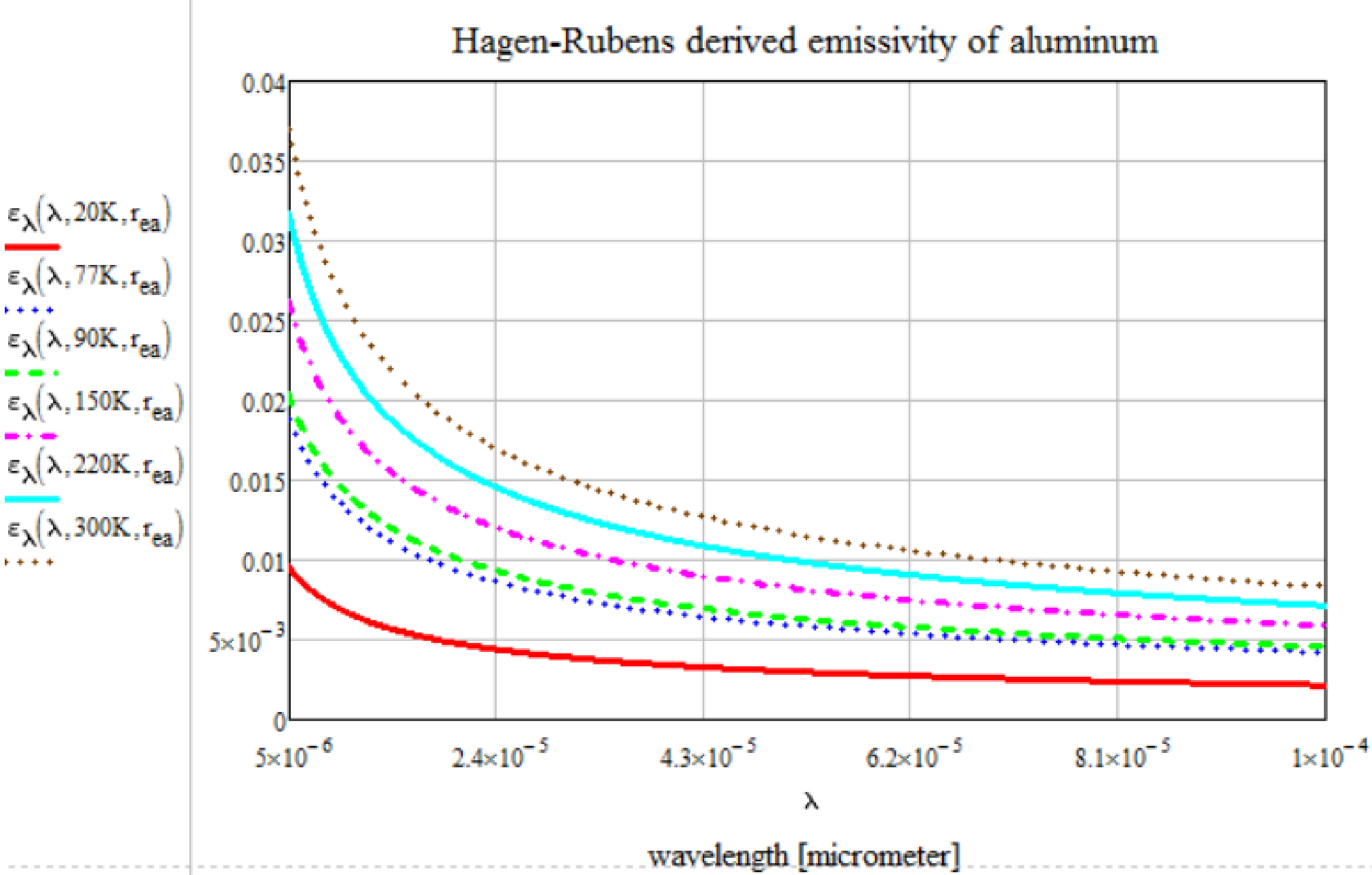

Predicted temperature dependent spectral emissivities as calculated with the two term Hagen-Rubens approximation.

Plotting flux as fxn of boundary temps

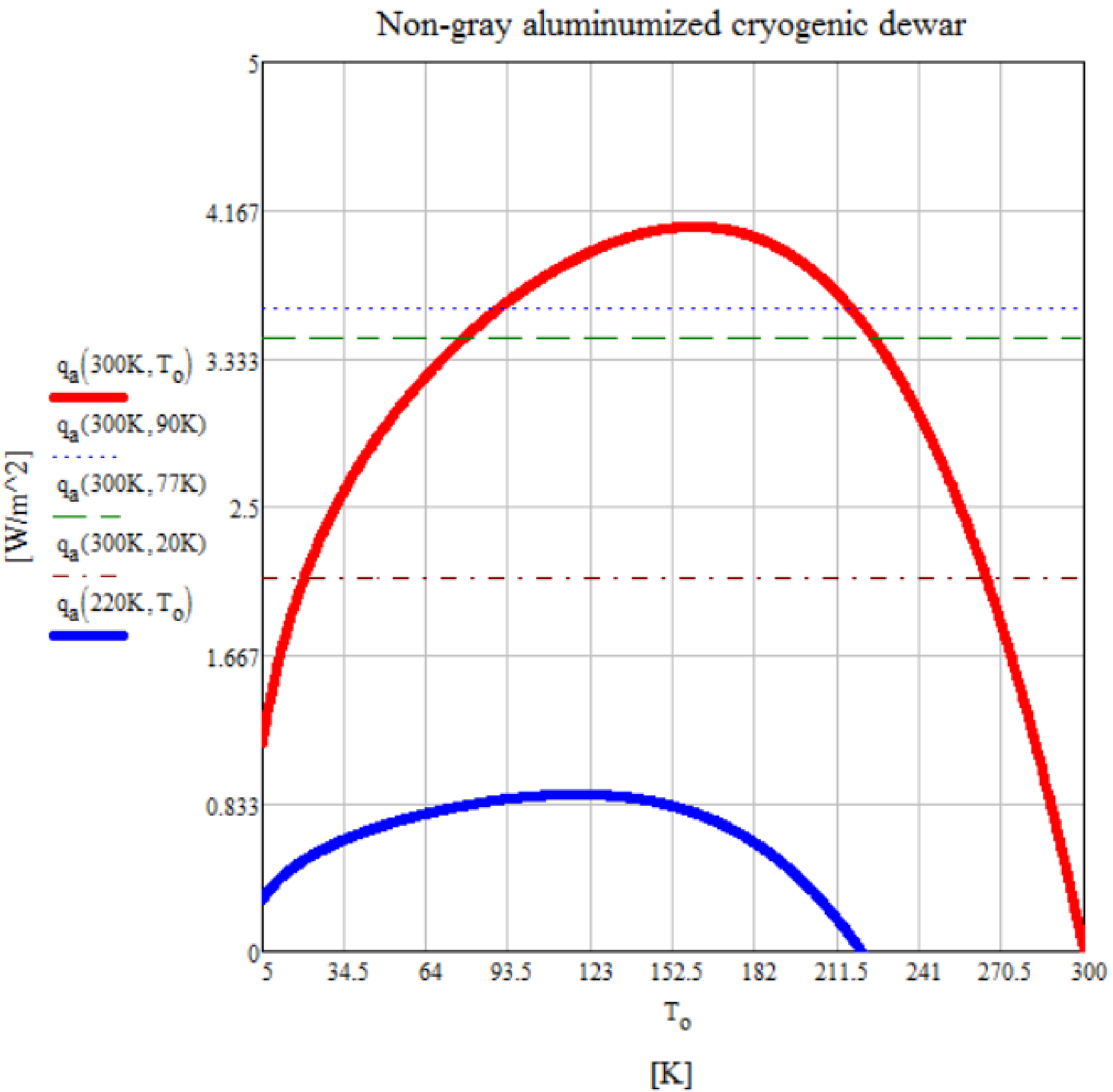

Paradox solved in Thermal Desktop

- Two concentric spheres, each with one boundary node
  - Outer boundary node at 300K, inner at either 77K (LN2) or 20K (LH2)
  - Radius 1m and 1.1m
- **Solution**:
  - 16.86 W @ LH2
  - **28.24 W @ LN2!!!**
  - **This works out to 68% increase, matching the expected results**

Bivariate Table Input

Enter values of Temperatures[K] on the first line
For additional lines, enter a single wavelengths[micro-m] followed by values of emissivity

	20	70	150	300
0	0.2	0.36	0.497	0.648
5	0.0096	0.018	0.026	0.037
10	0.0068	0.013	0.019	0.026

Non-gray MLI in the cryogenic regime

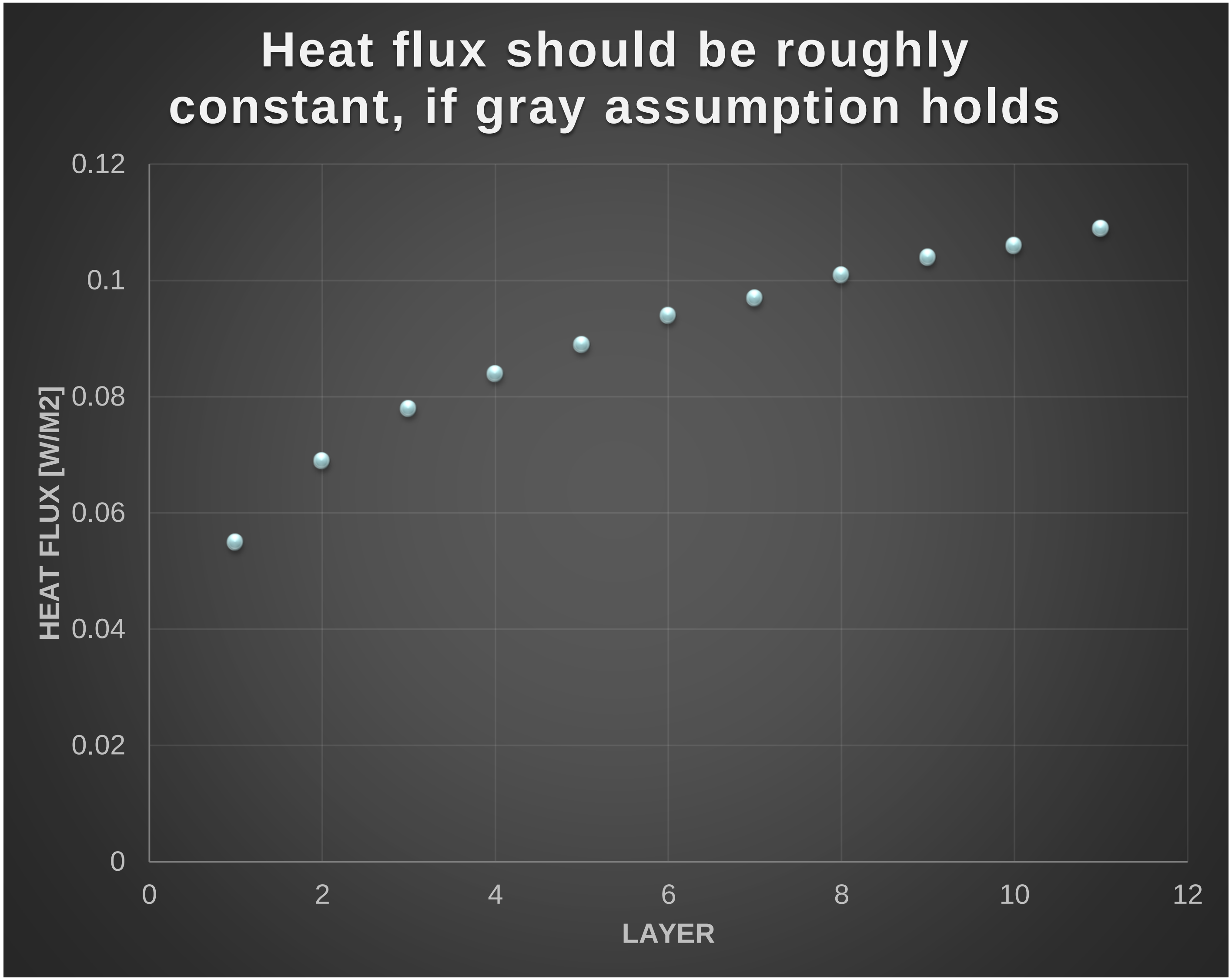

Is the gray assumption justified?

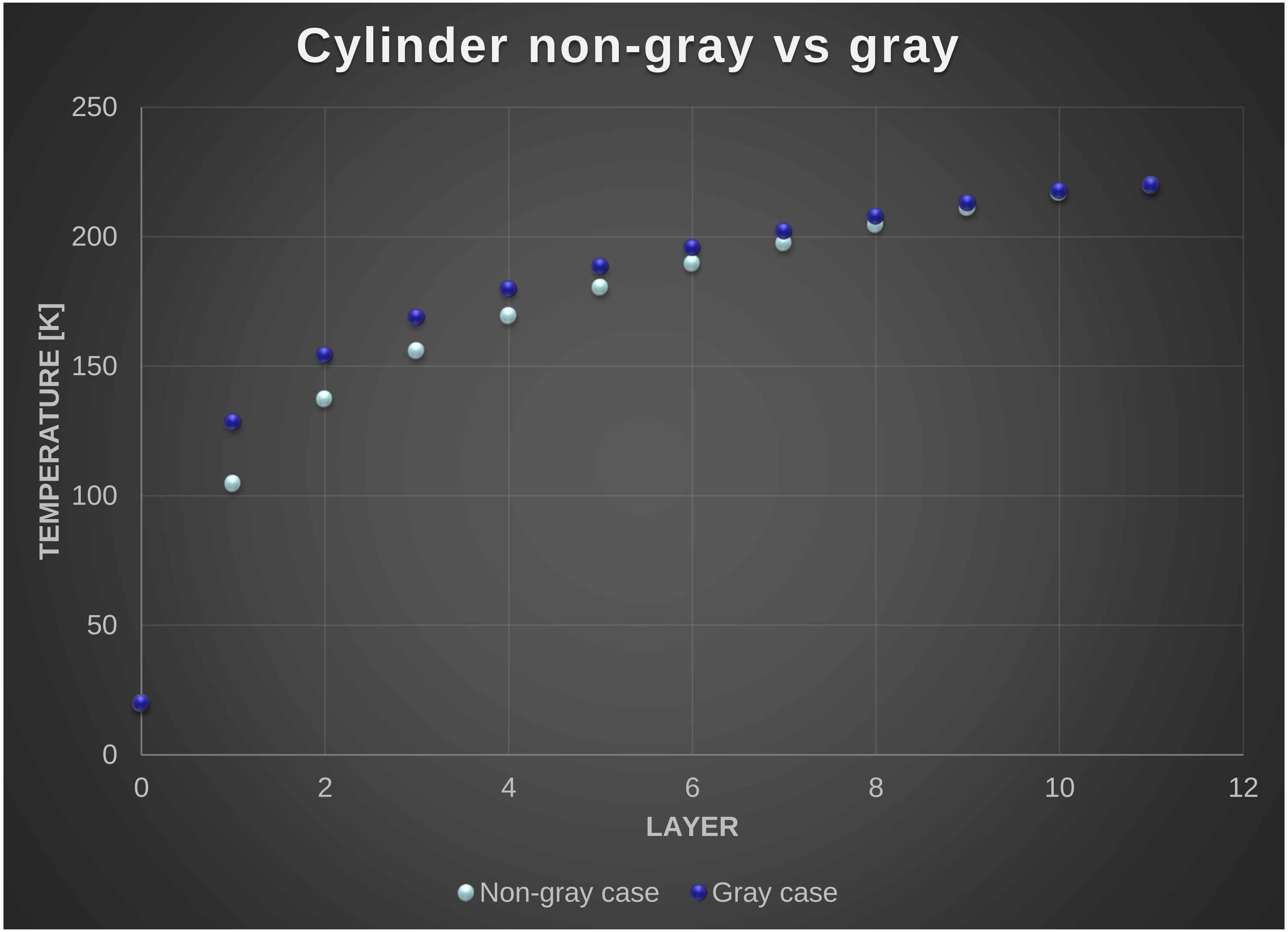

Modeling MLI with Thermal Desktop

- Inner cold surface area was 1 square meter
- Layer thickness 2.5x10^(-5) m
- Ten layers of insulation
- Layer spacing 1 mm
- Two fixed dirichlet (prescribed) conditions at 90K and 220K unless otherwise stated
- **1,000,000 rays (chosen after finding at least 100,000 rays were acceptable based on test runs)**
- Aluminized kapton, 1 mil, BOL with IR emissivity of 0.61 (inner surface matches this value), unless otherwise stated

Sample gradient with seam

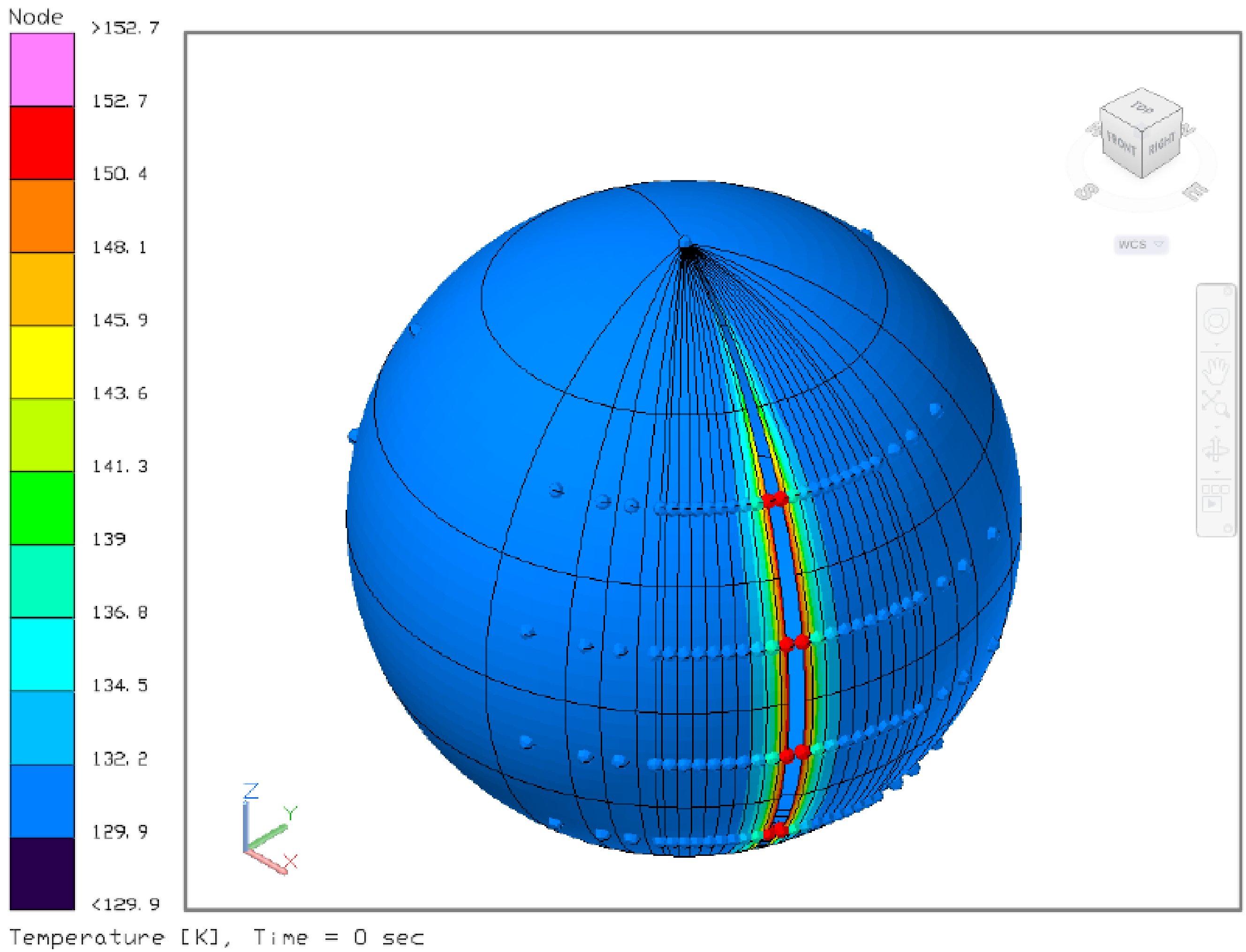

Heat flux changes with aspect ratio

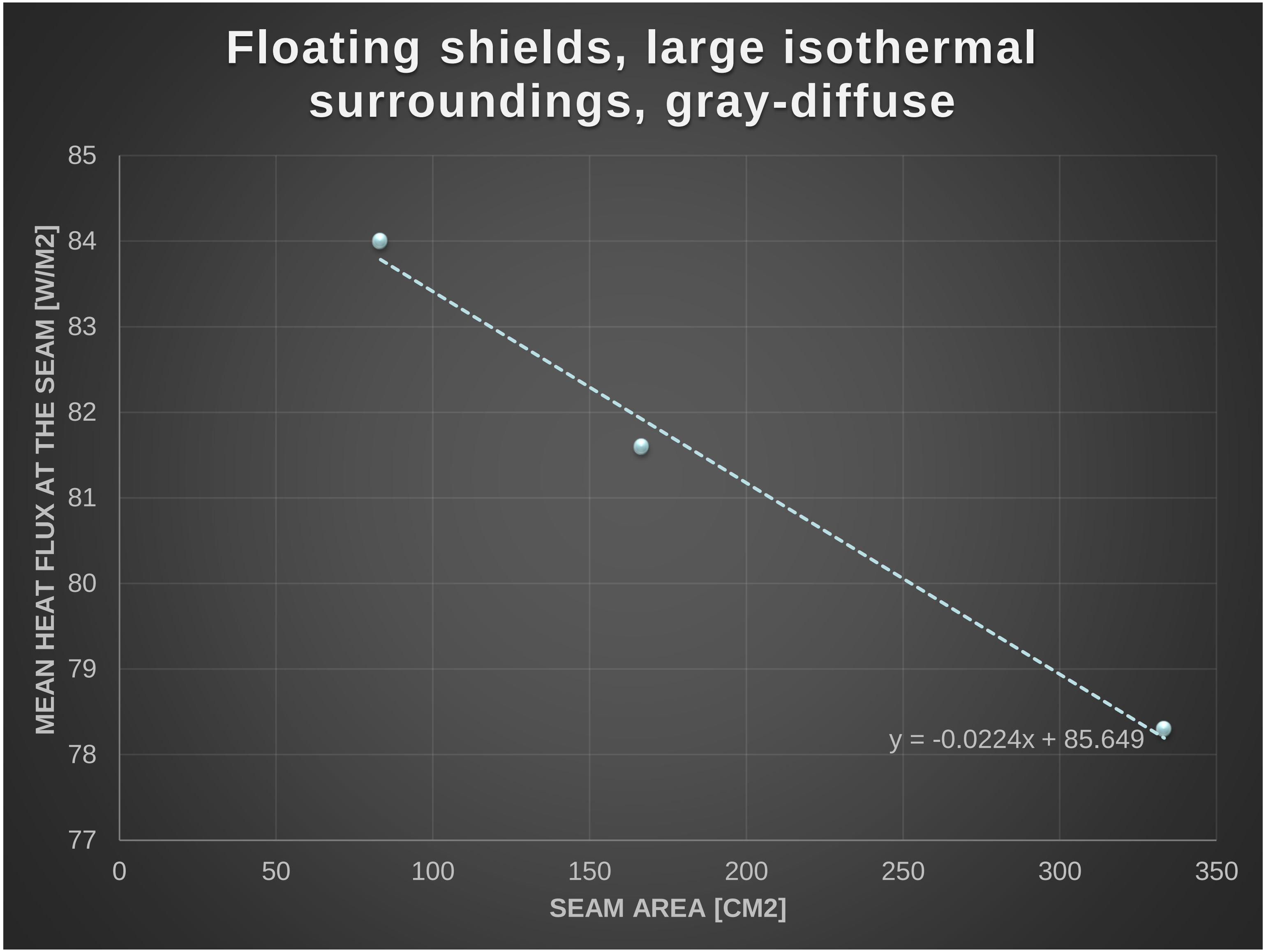

The effectiveness of using a patch

- Surroundings added as a very closely spaced surface near the outer layer of the MLI stack
- same emissivity of 0.61
- Resulting heat leak -5.78 W/m2
  - Close to ideal, floating shields case with no seams
  - Suggests that patching over seams ought to be very effective

Questions?

References

References

[1] J. Robert Branstetter. Radiant heat transfer between nongray parallel plates of tungsten. Technical report, 1961. Technical Note D-1088.

[2] Richard V. Cartwright. Multilayer insulations: a state of the art assessment. Technical report, 2011. Johns Hopkins University, Whiting School of Engineering.

[3] Brent Cullimore and Steven G. Ring et al. Thermal desktop user's manual. Technical Report Version 5.8, C & R Technologies, Jun 2015. CAD Based Thermal Analysis and Design.

[4] G.R. Cunnington, C.W. Keller, and G.A. Bell. Thermal performance of multilayer insulations. Technical Report NASA-CR-72605 & LMSC-A903316, Lockheed Missiles and Space Co., Apr 1971. Sunnyvale, Calif.

[5] G.R. Cunnington and C.L. Tien. A study of heat-transfer process in multilayer insulations. Number 69-607, San Francisco, California, June 1969.

AIAA 4th Thermophysics Conference, Lockheed Palo Alto Research Laboratory.

[6] G.R. Cunnington and C.L. Tien. A study of heat-transfer process in multilayer insulations. *AIAA Progress in Astronautics and Aeronautics*, pages 111–126, 1970. A portion of this study was conducted under NASA Contract NAS 3-12025, Lewis Research Center.

[7] G.R. Cunnington and C.L. Tien. A study of heat-transfer processes in multilayer insulations. In Jerry T. Bevans, editor, *Thermophysics: Applications to Thermal Design of Spacecraft*, pages 111–126. Academic Press, New York and London, 1970.

[8] Lady (editor) Dewar. *Collected papers of Sir James Dewar*, volume 1 and 2. Cambridge University Press, 1927.

[9] T. Echániz, R.B. Pérez-Sáez, and M.J. Tello. Optical properties of metals: infrared emissivity in the anomalous skin effect spectral region. *Journal of Applied Physics*, (116), 2014. 093508.

[10] M. M. Finckenor and D. D. Dooling. Multilayer insulation material guidelines. Technical Report TP-1999-209263, NASA, Apr 1998.

[11] David G. Gilmore, editor. *Spacecraft Thermal Control Handbook*, volume 1. The Aerospace Press, 2 edition, 2002.

[12] DeWitt Incropera, Bergman, and Lavine. *Fundamentals of Heat and Mass Transfer*. Wiley, 6 edition, 2007.

[13] Max Jakob, editor. *Heat transfer*, volume 1. Wiley, 1949.

[14] Lonny Kauder. Spacecraft thermal control coatings references. Technical Report NASA/TP-2005-212792, NASA, Dec 2005.

[15] C.W. Keller, G.R. Cunnington, and A.P. Glassford. Thermal performance of multilayer insulations. Technical Report NASA-CR-134477 & LMSC-D349866, Lockheed Missiles and Space Co., Apr 1974. Sunnyvale, Calif.

[16] C.W. Keller, G.R. Cunnington, and A.P. Glassford. Thermal performance of multilayer insulations. Technical Report NASA CR-134477, Lockheed Missiles & Space Company, Inc., Apr 1974.

[17] E.I. Lin, J.W. Stultz, and R.T. Reeve. Effective emittance for cassini multilayer insulation blankets and heat loss near seams. *J. of Thermophysics and Heat Transfer*, 10(2), 1996. April-June.

[18] Glen E. McIntosh. Layer by layer mli calculation using a separated mode equation. Cryogenic Engineering Conference, 1993.

[19] T. Ohmori, A. Yamamoto, and M. Nakajima. The effect of non-zero thermal radiation transmissivity of the aluminized mylar film on the thermal performance of super-insulation. *Advances in Cryogenic Engineering: Proceedings of the Cryogenic Engineering Conference*, pages 1573–1582, 1960.

[20] Ron Ross. Calculation of the thermal radiation properties of low-emissivity surfaces at temperatures below 50 k. 2006. Unpublished draft available by request.

[21] Q.S. Shu. Systematic study to reduce the effects of cracks in multilayer insulation part 1: theoretical model. *Cryogenics*, 27:249–256, May 1987. Fermi National Accelerator Laboratory.

References

[22] Q.S. Shu, R.W. Fast, and H.L. Hart. Systematic study to reduce the effects of cracks in multilayer insulation part 2: experimental results. *Cryogenics*, 27:298–311, June 1987.

[23] Robert Siegel and John R. Howell. *Thermal Radiation Heat Transfer*. Hemisphere Publishing Corporation, 3 edition, 1992.

[24] J. Srinivasan. A paradox in radiation heat transfer. *AIP Advances*, pages 85–91, 2007. Centre for Atmospheric and Oceanic Sciences and Mechanical Engineering, Indian Institute of Science.

[25] C.L. Tien. A correlation for thermal contact conductance of nominally flat surfaces in vacuum. pages 755–759. Proceedings of the Seventh Thermal Conductivity Conference, September 1968. NBS SP-302.

[26] C.L. Tien and G.R. Cunnington. Cryogenic insulation heat transfer. *Advances in Heat Transfer*, 9:349–417, 1973.

[27] I.A. Black & Glaser "Progress report on development of high-efficiency insulation," (Advances in Cryogenic Engineering volume 6, proceedings of the 1960 Cryogenic Engineering Conference)

Backup

Table 1. Superinsulation System Equations

Double-Aluminized Mylar-Silk Netting (2 layers)	$k_e = 1.13\times10^{-9}\bar{N}\,T_m + \frac{\sigma\,(T_h^2+T_c^2)\,(T_h+T_c)\,t}{(N-1)[(2/\epsilon)-1]}$
NRC-2	$k_e = 5.90\times10^{-12}(\bar{N})^2\,T_m + \frac{\sigma\,(T_h^2+T_c^2)\,(T_h+T_c)\,t}{(N-1)\,[(1/\epsilon_a)+(1/\epsilon_b)-1]}$
Superfloc	$k_e = 3.23\times10^{-11}(\bar{N})^2\,T_m + \frac{\sigma\,(T_h^2+T_c^2)\,(T_h+T_c)\,t}{(N-1)\,[(1/\epsilon_a)+(1/\epsilon_b)-1]}$
Double-Aluminized Mylar-Nylon Net (1 layer)	$k_e = 6.0\times10^{-11}(\bar{N})^{1.4}\,T_m + \frac{\sigma\,(T_h^2+T_c^2)\,(T_h+T_c)\,t}{(N-1)\,[(2/\epsilon)-1]}$
Double-Aluminized Mylar-Dexiglas	$k_e = 4.58\times10^{-12}\,(\bar{N})^2\,T_m + \frac{2.7\,\sigma\,(T_h^2+T_c^2)\,(T_h+T_c)\,t}{(N-1)\,[(2/\epsilon)-1]}$
Dougle-Aluminized Mylar-Tissuglas	$k_e = 1.83\times10^{-12}(\bar{N})^2\,T_m + \frac{1.7\,\sigma\,(T_h^2+T_c^2)(T_h+T_c)\,t}{(N-1)[(2/\epsilon)-1]}$
Dougle-Aluminized Crinkled Mylar-Tissuglas	$k_e = 4.6\times10^{-12}\,(\bar{N})^2\,T_m + \frac{1.7\,\sigma\,(T_h^2+T_c^2)\,(T_h+T_c)\,t}{(N-1)[(2/\epsilon)-1]}$
Double-Aluminized Mylar-Open-Cell Foam	$k_e = 1.26\times10^{-14}\,(\bar{N})^{5.1}\,T_m + \frac{\sigma\,(T_h^2+T_c^2)(T_h+T_c)\,t}{(N-1)\,[(2/\epsilon)-1]}$
Double-Aluminized Mylar-Closed-Cell Foam	$k_e = 3.5\times10^{-15}\,(\bar{N})^{5.7}\,T_m + \frac{\sigma\,(T_h^2+T_c^2)(T_h+T_c)\,t}{(N-1)\,[(2/\epsilon)-1]}$

k_e = effective thermal conductivity
$\bar{N}$ = no. of radiation shields/unit thickness
T_m = mean temperature
σ = Stefan Boltzmann constant
T_h = hot temperature
T_c = cold temperature
N = no. of radiation shields
t = thickness of insulation
ϵ = emissivity

Simulating infinite parallel planes using reflecting surfaces

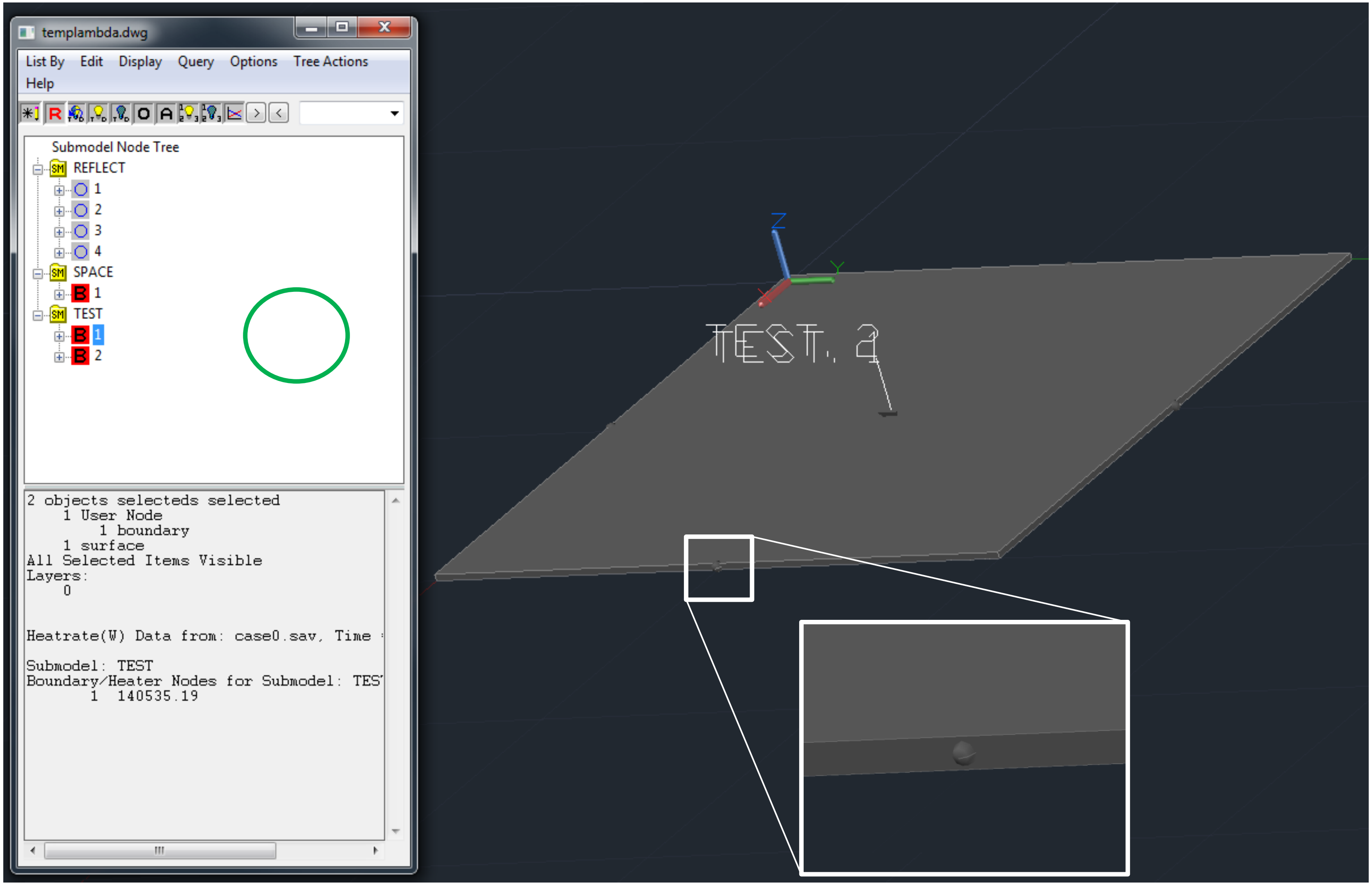

Adding contact conductance

- Contacting shields, 3 degree opening, large isothermal surroundings, gray-diffuse
  - Contact conductance 0.05 W/m2/K
  - Resulting heat leak -6.66 W/m2 (roughly 10% more than floating)

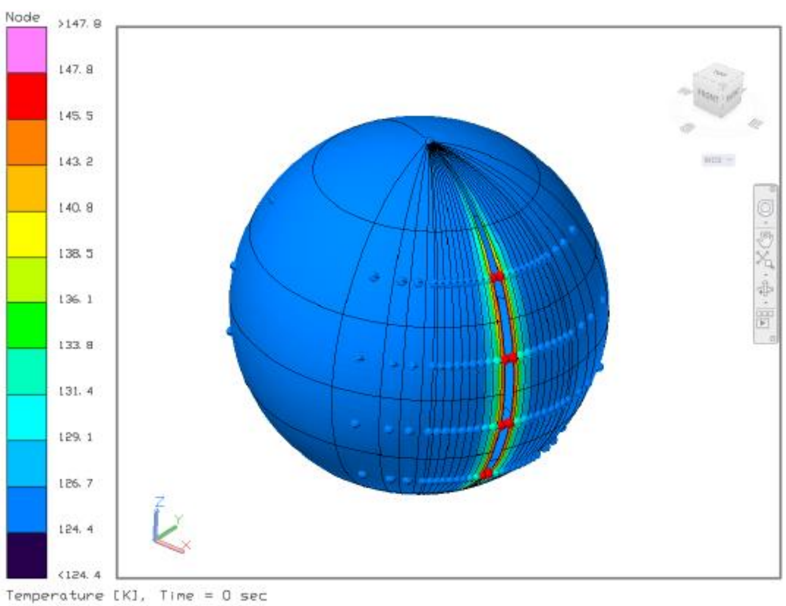

Figure 75: Case 7, layer 1.

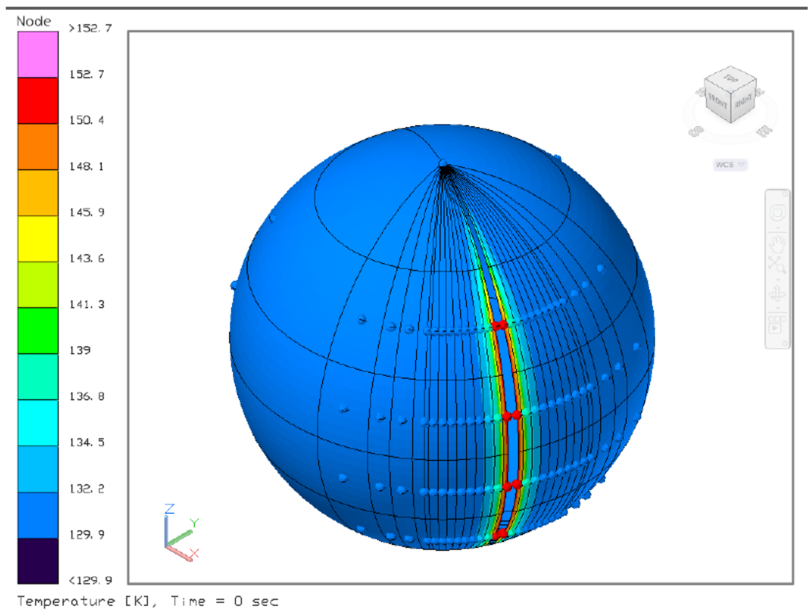

Figure 41: Case 1, layer 1.

- Contact conductance increased by order of magnitude to 0.5 W/m2/K
  - Resulting heat leak -11.97 W/m2

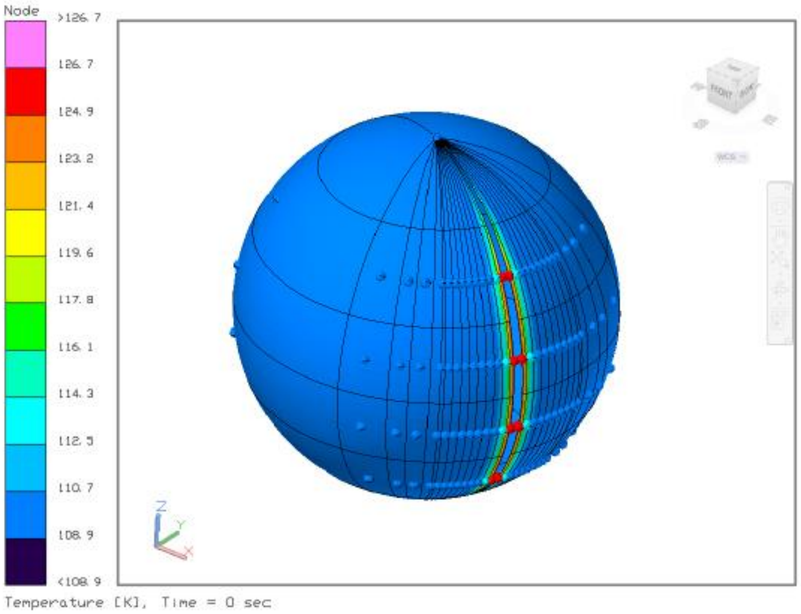

Figure 86: Case 8, layer 1.

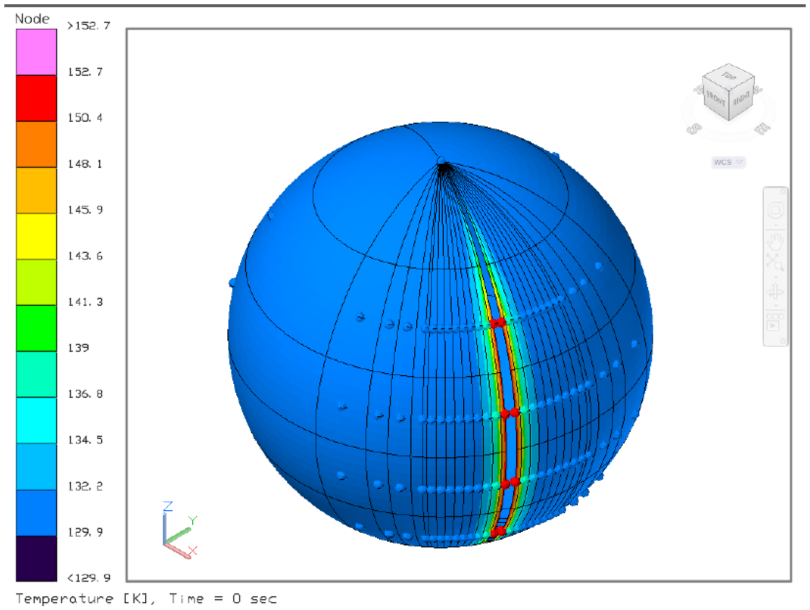

Figure 41: Case 1, layer 1.

Thermal radiation occurs between 10^{-1} µm and 10^{2} µm. This encompasses part of the ultraviolet spectrum, the entire visible light spectrum, and the entire infrared spectrum. To understand thermal radiation, the concept of the blackbody and its properties should be defined as follows.

1. A blackbody absorbs all incident radiation, regardless of wavelength and direction
2. For a prescribed temperature and wavelength, no surface can emit more energy than a blackbody.
3. Although the radiation emitted by a blackbody is a function of wavelength and temperature, it is independent of direction. That is, the blackbody is a diffuse emitter.

The blackbody spectral intensity is well known, having first been determined by Plank[4].

$$I_{\lambda_b}(\lambda, T) = \frac{2hc_o^2}{\lambda^5(e^{\frac{hc_o}{\lambda kT}}) - 1} \tag{2}$$

Since the blackbody is by definition a diffuse emitter, it follows that the spectral emissive power, after integration, is simply the spectral intensity multiplied by π.

$$E_{\lambda_b}(\lambda, T) = \pi I_{\lambda_b}(\lambda, T) \tag{3}$$

An example of the Plank distribution plotted for a temperature of 20K is shown in 2.

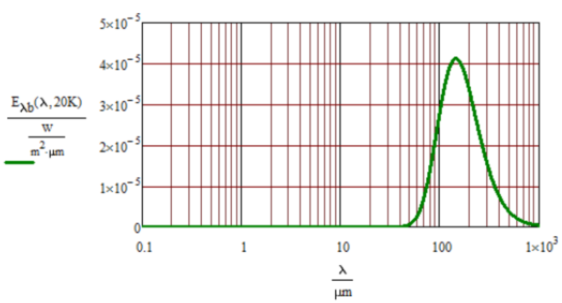

Figure 2: The famous Plank blackbody distribution, showing the emission spectrum for some blackbody at a temperature of 20K. This curve will shift to the left as the temperature of the blackbody increases.

By integrating 3 over the wavelength from zero to infinity, the Stefan-Boltzmann Law is obtained.

$$E_b(T) = \sigma T^4 \tag{5}$$

$$\Gamma_{\alpha_\beta}(\alpha, \beta, T) = \int_\alpha^\beta \frac{E_{\lambda_b}(\lambda, T)}{\sigma T^4} d\lambda \tag{6}$$

As an example, for 90K, considering a band up to 250 µm would account for 99% of the energy emitted. For 220K, a band up to 102 µm needs to be considered to account for 99% of the energy (these results are shown in Figure 3).

Relevant to cryogenic superinsulation heat transfer, consider that, in Figure 3, less than 1% of the energy is in the band from 250 µm to 1000 µm for the 90K case. The wavelength here is on the order of the spacing of the insulation (roughly 10 layers per centimeter means layer spacing is on the order of 0.1 cm

$$F_{\lambda 1\_to\_\lambda 2}(\lambda_1, \lambda_2, T) := \int_{\lambda_1}^{\lambda_2} \frac{E_{\lambda b}(\lambda, T)}{\sigma \cdot T^4} d\lambda$$

$$F_{\lambda 1\_to\_\lambda 2}(0\mu m, 250\mu m, 90K) = 0.99058435978$$
$$F_{\lambda 1\_to\_\lambda 2}(0\mu m, 102\mu m, 220K) = 0.99050727574$$
$$F_{\lambda 1\_to\_\lambda 2}(250\mu m, 1000\mu m, 20K) = 0.352060993733$$
$$F_{\lambda 1\_to\_\lambda 2}(1000\mu m, 10000\mu m, 20K) = 0.014433547225$$
$$F_{\lambda 1\_to\_\lambda 2}(0\mu m, 250\mu m, 2K) = 0.000000001308$$
$$F_{\lambda 1\_to\_\lambda 2}(250\mu m, 1000\mu m, 2K) = 0.066875394433$$
$$F_{\lambda 1\_to\_\lambda 2}(1000\mu m, 10000\mu m, 2K) = 0.919737281264$$

Figure 3: A computer algebra system, like MathCAD, is very useful to avoid the table lookup typically associated with band fractions.

which equals 1000 µm). At 20K, the energy in the 250 µm to 1000 µm band jumps drastically to 35%, with 1% of the energy having a wavelength between 1000 µm and 10 000 µm, which is greater than the spacing the layers. At 2K, 92% of the energy has a wavelength in this very long band from 1000 µm and 10 000 µm which is equivalent to 0.1 cm and 1 cm.

Srinivasan math

$$\varepsilon_{\lambda n}(\lambda, t, r_{e273}) := 36.5\cdot\left(\frac{\mu m}{\Omega\cdot cm}\right)^{\frac{1}{2}}\cdot\left(\frac{\frac{r_{e273}}{273K}\cdot t}{\lambda}\right)^{\frac{1}{2}} - 464\cdot\left(\frac{\mu m}{\Omega\cdot cm}\right)\cdot\frac{\frac{r_{e273}}{273K}\cdot t}{\lambda}$$

$$C_1 := 3.742\cdot 10^{8}\,\frac{W\cdot(\mu m)^4}{m^2} \qquad C_2 := 1.439\cdot 10^{4}\,\mu m\cdot K$$

$$e_b(\lambda, T_o) := \frac{C_1}{\lambda^5\cdot\left(e^{\frac{C_2}{\lambda\cdot T_o}} - 1\right)}$$

$$\varepsilon_{\lambda h}(\lambda, t, r_{e273}) := 1.3\cdot\varepsilon_{\lambda n}(\lambda, t, r_{e273})$$

$$\varepsilon_{\lambda ha}(\lambda, t) := \varepsilon_{\lambda h}\left(\lambda, t, 2.82\cdot 10^{-6}\,\Omega\cdot cm\right)$$

$$q_a(T_1, T_2) := \int_5^{10000} \frac{\left(e_b(\lambda\cdot\mu m, T_1) - e_b(\lambda\cdot\mu m, T_2)\right)}{\frac{1}{\varepsilon_{\lambda ha}(\lambda\cdot\mu m, T_1)} + \frac{1}{\varepsilon_{\lambda ha}(\lambda\cdot\mu m, T_2)} - 1}\, d\lambda\cdot\mu m$$

$$q_a(300K, 90K) = 3.616\cdot\frac{W}{m^2}$$

$$q_{ratioa} := \frac{q_a(300K, 77K)}{q_a(300K, 20K)} = 1.637$$

Figure 21: Solution to the nongray dewar problem following the approach of Srinivasan [24] which keeps a two term approximation of the Hagen-Rubens relation.